Numerical study of heat transfer in Sakiadis flow involving Maxwell fluid

by

Shawana Maryum

A thesis submitted in partial fulfillment of the requirements
for the degree of Master of Science in Mathematics

Supervised by

Dr. Meraj Mustafa Hashmi

School of Natural Sciences,
National University of Sciences and Technology,
Islamabad, Pakistan

2019

FORM TH-4

National University of Sciences & Technology

MS THESIS WORK

We hereby recommend that the dissertation prepared under our supervision by: Shawana Maryum, Regn No. 00000172958 Titled: **Numerical study of heat transfer in Sakiadis flow involving Maxwell fluid** accepted in partial fulfillment of the requirements for the award of **MS** degree.

Examination Committee Members

1. Name: DR. MUJEEB UR REHMAN Signature: _____

2. Name: DR. AMMAR MUSHTAQ Signature: _____

External Examiner: PROF. MUHAMMAD AYUB Signature: _____

Supervisor's Name DR. MERAJ MUSTAFA HASHMI Signature: _____

_____ 30-8-19.
Head of Department Date

COUNTERSINGED

Date: 30/8/2019

Dean/Principal

THESIS ACCEPTANCE CERTIFICATE

Certified that final copy of MS thesis written by **Ms. Shawana Maryum** (Registration No. **00000172958**), of **School of Natural Sciences** has been vetted by undersigned, found complete in all respects as per NUST statutes/regulations, is free of plagiarism, errors, and mistakes and is accepted as partial fulfillment for award of MS/M.Phil degree. It is further certified that necessary amendments as pointed out by GEC members and external examiner of the scholar have also been incorporated in the said thesis.

Signature: _____

Name of Supervisor: Dr. Meraj Mustafa Hashmi

Date: 30-08-19

Signature (HoD): _____

Date: 30-8-19

Signature (Dean/Principal): _____

Date: 30/8/2019

Dedicated to my parents for their constant support,

to my brothers for always encouraging me and to

Amna Sadiq for always being there for me.

Acknowledgment

In the Name of Allah, The Most Beneficent, The Merciful. All the praise to His Prophet Muhammad (Peace be upon him), who gave us vision, wisdom and courage to complete this thesis.

Firstly, I would like to express my deepest and sincerest gratitude for my supervisor Dr. Meraj Mustafa Hashmi. Without his constant support and enlightenment, this thesis would not have been possible. I would like to extend my gratitude to my G.E.C members, Dr. Mujeeb ur Rehman and Dr. Ammar Mushtaq for their guidance and help whenever I needed it.

My parents have catered my every need as well as my every want. It is their love and prayers that has enabled me to achieve this milestone. I am eternally in their debt. My brothers have been my constant supporters in all that I did.

Lastly, I would like to acknowledge the administration staff as well the helpers at my department for helping me whenever I needed their assistance.

Contents

1. Introduction **1**

1.1 Background 1

1.2 Some dimensionless numbers 3

1.2.1 Reynolds number 3

1.2.2 Prandtl number 3

1.2.3 Nusselt number 3

1.2.4 Deborah number 4

1.2.5 Biot number 4

1.2.6 Magnetic interaction parameter 4

1.3 Preliminary concepts 5

1.3.1 Boundary layer 5

1.3.2 Non-Newtonian fluids 6

1.3.3 Thermal conductivity 8

1.3.4 Electrical conductivity 9

1.3.5 $bvp4c$ 9

2. Numerical study for Sakiadis flow of MHD Maxwell fluid with variable thermal conductivity **10**

2.1 Problem formulation 10

2.2 Numerical method 13

2.3 Numerical results and discussion 13

2.4 Concluding remarks 20

3. Numerical study for Sakiadis flow of MHD Maxwell fluid inspired by nonlinear radiation heat flux 21

3.1 Problem formulation 21

3.2 Numerical method 24

3.3 Results and discussion 24

3.4 Concluding remarks 32

References **32**

Abstract

A fluid for which stress isn't linearly related to deformation rate is termed as a non-Newtonian fluid. Such fluids help us comprehend the widespread variety of fluids that occur in the physical world. Many researchers explored non-Newtonian fluids via upper-convected Maxwell model which is preferred due to its wide-ranging applications.

Chapter 1 includes a brief background of the research undertaken in this thesis. Dimensionless numbers and their significance are described briefly. Some important concepts employed in the thesis are explained.

Chapter 2 focuses on variable thermal conductivity effects on a viscoelastic fluid flow past a continuously flat plate placed in stationary fluid subjected to convective heating. A convenient routine bvp4c of MATLAB is invoked to find similarity solutions. The role of variable thermal conductivity on temperature is clarified by plotting graphs.

Chapter 3 concerns with radiation effects on viscoelastic fluid flow around a moving flat plate in an otherwise calm environment. Analysis is based on physically realizable convective type condition and inclusion of wall suction. Moreover, nonlinear Rosseland formula for radiative heat flux is utilized. Using Similarity approach, the velocity and temperature profiles are estimated numerically for wide range of viscoelastic fluid parameter.

Chapter 1

Introduction

1.1 Background

Heat transfer in non-Newtonian fluids has been an area of great interest for fluid dynamics research community. Non-Newtonian fluid models give flow description of liquids generally faced in natural surroundings and industries, for instance biological fluids, foams, liquids with polymers, slurries etc. Unlike water and air, these fluids possess at least one rheological feature out of shear-thinning/thickening, nonlinear creep, normal stress differences, stress relaxation or yielding. Although, viscoelastic fluids act as viscous fluids in long-time experiments but their initial response to the applied stress is like that of elastic solid. Maxwell model is perhaps the widely accepted model that explains the stress-relaxation feature of viscoelastic materials. Numerous industrial processes involve non-Newtonian fluid flow around moving belts or plates. A few noteworthy examples are spinning of artificial fiber, paper production, thread travelling in amid a windup roll and feed roll, cooling of a long metallic plate, continuous casting, glass manufacturing etc. Such flows usually comprise of boundary layer flow problem caused either by fluid flow prompted due to uniform flow across a flat fixed plate, or by the flow triggered by a moving flat plate in an otherwise stationary fluid. The formerly mentioned flow type is known infamously as Blasius flow and the later as Sakiadis flow. Flow above a plate as well as a sheet was initially investigated by authors Blasius [1] and Sakiadis [2, 3] in the earlier times i.e. 19^{th} century. Sadeghy et al. [4] tested different approaches for Sakiadis flow of viscoelastic fluid obeying Maxwell model. Later, Kumari and Nath [5] made use of Maxwell model to analyze buoyancy induced viscoelastic fluid flow exposed to transverse magnetic field. Hayat et al. [6] formulated and resolved stagnation point flow of Maxwell fluid impinging on a horizontal surface by analytical method. Shateyi [7] resolved flow past a vertical stretchable surface placed in an incompressible Maxwell fluid containing chemically reactive species. Mustafa [8] elucidated non-Fourier heat flux in rotating viscoelastic fluid above a stretching surface utilizing homotopy analysis method. Later, Abbasi and Shehzad [9] also conducted non-Fourier heat transfer analysis for viscoelastic fluid flow resulted due to bidirectional stretching of an elastic surface. Later, Hsiao [10] explored radiative heat transfer in viscoelastic fluid flow bounded by

an extensible surface. Similar boundary layer problems concerning Maxwell fluid are published frequently in recent times [11-17].

Heat transfer simply put is transfer of energy whenever in a medium temperature difference exists. Convective heat transfer take place between a surface and moving fluid kept at different temperatures. A consequence of the fluid-surface interaction is the development of a boundary layer where the velocity changes from zero at the boundary i.e. $y = 0$ to a finite value U_∞. Moreover temperature difference between fluid and surface results in the formation of thermal boundary layer, where temperature varies from T_w at the boundary to T_∞ in the free streamline. In the case when $T_w > T_\infty$, convective heat transfer occurs from the surface to the outer flow. Many researchers also showed interest in forced convection caused due to an application of heat source to the boundary layer flow. On the other hand, radiative heat transfer is imperative in astrophysical flows, nuclear reactor cooling, solar power technology, electrical power generation, cooling of electronic devices and energy production etc. In most of the earlier articles, the practice was to linearize Rosseland heat flux by utilizing the assumption of small temperature difference. (See, for instance, Refs. [18-22]). Magyari [23], in 2011, revealed that the use of linearized Rosseland formula for radiation doesn't add any novelty keeping in view the computational of physical perspective of the problems. Pantokratoras and Fang [24], [25] investigated the effects of nonlinear Rosseland thermal radiation on the Sakiadis and Blasius flow. Motivated by [23], flow analysis by using non-linear radiative heat flux has been considered in many recent articles. Pal et al. [26] investigated the impact of nonlinear radiation on MHD mass and heat transfer in a thin liquid film. Hayat et al. [27] addressed the coinciding characteristics of nonlinear thermal radiation and melting heat transfer effects in stagnation point flow of carbon nanotubes due to stretching cylinder. Effects of heat generation/absorption along a moving slip surface with nonlinear thermal radiation were studied by Soomro et al. [28]. Reddy et al. [29] considered the flow of a nanofluid over a curved shaped stretchable geometry and carried out the numerical study of heat and mass transfer by assuming nonlinear radiation. Mustafa et al. [30] dealt with the nonlinear radiative heat flux in laminar flow due to rough rotating disk in the presence of partial slip effects and vertical magnetic field. Some more recent work carried out in this area is given through [31-37].

Motivation of current thesis is twofold. Firstly, to consider variable thermal conductivity for a viscoelastic fluid flow around a convectively heated wall. Such problem comprises of a nonlinear boundary condition which is not yet reported in the literature. Secondly, the aspect of nonlinear radiation in Sakiadis flow of viscoelastic fluid. The numerical solutions of above problems are sought by a contemporary MATLAB solver bvp4c, the details of which can be found from [38] and [39].

1.2 Some dimensionless numbers

1.2.1 Reynolds number

Reynolds numbers (Re) is used to predict whether the flow is laminar or turbulent. Mathematically, the ratio of inertial forces to viscous forces defines Reynolds number, given by:

$$Re = \frac{\rho v L}{\mu} = \frac{v L}{\nu}. \tag{1.1}$$

where L is the characteristic length and $\nu = \mu/\rho$ is termed kinematic viscosity. At low Reynolds number, viscous forces relatively dominate thereby producing laminar flow. On the other hand, inertial forces dominate at high Reynolds number and thus initiate turbulence in fluid flow.

1.2.2 Prandtl number

Prandtl number (Pr) is used to determine heat transfer between a moving fluid and a solid surface. Mathematically, it is the ratio of momentum diffusion to thermal diffusion, represented as:

$$Pr = \frac{\nu}{\alpha} = \frac{c_p \mu}{\kappa}, \tag{1.2}$$

where $\alpha = \kappa/\rho c_p$ denotes the thermal diffusivity in which κ is thermal conductivity and c_p represents the specific heat capacity.

1.2.3 Nusselt number

The ratio of convective heat transfer to conductive heat transfer defines Nusselt number. Mathematically:

$$\text{Nusselt number} = \frac{h}{\kappa/L}, \tag{1.3}$$

where h is the convective heat transfer coefficient.

1.2.4 Deborah number

A viscoelastic parameter used to characterize the fluidity of material under explicit flow environments is known as Deborah number. In mathematical terms, it is the ratio between two time quantities, which are, time required by the material to adjust to applied stress and the characteristic time for which the stress was applied, represented as:

$$\text{Deborah number} = \frac{t_c}{t_p}, \tag{1.4}$$

where t_c denotes relaxation time and t_p represents the time of observation. At low Deborah number, material tends to be more fluid like and at high values, it acts more solid like.

1.2.5 Biot number

Biot number analyzes the interaction between conduction in a solid and convection at the solid's surface. Mathematically,

$$Bi = \frac{h}{\kappa}\sqrt{\frac{\nu}{U}}, \tag{1.5}$$

where U is the horizontal velocity of the plate.

1.2.6 Magnetic interaction parameter

It is a parameter of prime importance when the flow is exposed to a transverse magnetic field being applied externally. Mathematically, it is the ratio of electromagnetic force to the viscous force, represented as:

$$M = \sqrt{\frac{\sigma B^2}{\rho U}}, \tag{1.6}$$

where σ denotes electrical conductivity, B is magnetic field intensity, ρ represents fluid density and U is horizontal velocity of the plate.

1.3 Preliminary concepts

1.3.1 Boundary layer

Boundary layer refers to the layer of fluid surrounding the boundary where the effect of the viscosity is present. Two important types of boundary layers are discussed below:

Momentum boundary layer

When fluid particles come in contact with a solid surface, they exhibit a zero velocity in order to adhere to the no-slip condition. These fluid particles impact the particles of the adjacent fluid layer and it consequentially influences the next layer fluid particles. This slowing of velocity goes on till a considerable distance from the flat surface is achieved where the retardation effect becomes negligible. In the boundary layer, fluid velocity varies from zero to $0.99U_\infty$, where U_∞ represents free stream velocity.

Thermal boundary layer

Thermal boundary layer forms when there is a temperature difference between the fluid flow and the surface across which the flow is flowing. This is the region where the temperature varies along $y-$ direction i.e. normal to the surface (as in Fig. 1.1).

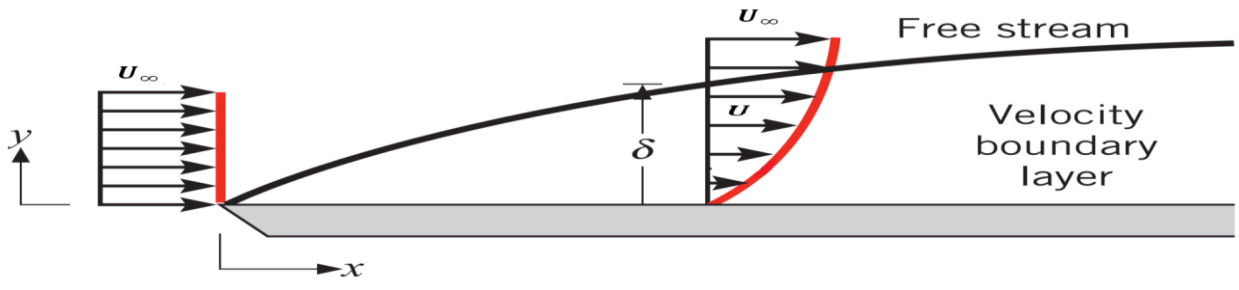

Figure 1.1: Boundary layer schematic

There are two well-known boundary layer flows. They are defined under:

Blasius flow refers to the fluid flow occurring over a stationary flat plate (at zero incidence) placed in a moving fluid. On the other hand, fluid flow triggered by a moving plate in an otherwise stationary fluid is termed as Sakiadis flow. Both Blasius and Sakiadis flow are described by the following equations:

$$\frac{\partial u}{\partial x}+\frac{\partial v}{\partial y}=0\,, \tag{1.7}$$

$$\rho\left(u\frac{\partial u}{\partial x}+v\frac{\partial u}{\partial y}\right)=\mu\frac{\partial^2 u}{\partial y^2}, \tag{1.8}$$

with u and v representing velocities in the $x-$ and $y-$ directions respectively where coordinate x is measured along the plate and y is normal to it. The boundary conditions are:

Blasius flow: $u(x,0)=v(x,0)=0,$ (1.9)

$$u\to U_\infty \quad \text{as} \quad y\to\infty.$$

Sakiadis flow: $u(x,0)=U,\ v(x,0)=0,$ (1.10)

$$u\to 0 \quad \text{as} \quad y\to\infty.$$

1.3.2 Non-Newtonian fluids

Fluids which do not adhere to Newton's law of viscosity are classified as non-Newtonian fluids. For these fluids, shear stress and deformation rate cannot be linked linearly. Under stresses, such fluids change their viscosity with varying strain rate. The flows involving non-Newtonian fluids prevail in a wide spectrum of applications in industrial processes such as synthetic fibers, polymer solutions, paper production etc. A vast variety of biological as well as industrial fluids exhibit non-Newtonian behavior, for example, blood, printer ink, ketchup, slurries and grease etc.

Since there doesn't exist a linear relation between stress and deformation rate, a single model cannot be used to define non-Newtonian fluids. Researchers have developed numerous models to study non-Newtonian fluids. Some widely used models include power-law model, Bird-Carreau model, Cross-Power law model, Herschel-Bulkey model, second-grade model etc. Somewhat

widely accepted and utilized model is the upper-convected Maxwell model. It is able to explain the memory effect exhibited by non-Newtonian fluids in terms of relaxation time.

The basic flow equations governing the Maxwell fluid flow are given under.

Governing equations for boundary layer flow of Maxwell fluid

Equations governing incompressible MHD Maxwell fluid flow are:

$$\boldsymbol{\nabla}.\boldsymbol{V} = 0, \tag{1.8}$$

$$\rho\left[\frac{d\boldsymbol{V}}{dt}\right] = -\boldsymbol{\nabla}p + \boldsymbol{\nabla}.\boldsymbol{S} + (\boldsymbol{J}\times\boldsymbol{B}), \tag{1.9}$$

where $\boldsymbol{V} = \big(u(x,y,z), v(x,y,z), w(x,y,z)\big)$ is the velocity vector, ρ is fluid density, d/dt is material derivative, $\boldsymbol{S}$ is extra stress tensor, $\boldsymbol{J}$ represents current density and $\boldsymbol{B} = \boldsymbol{B} + \boldsymbol{B_i}$ is the total magnetic field. $\boldsymbol{B_i}$ is induced magnetic field which is neglected by assuming small magnetic Reynold's number.

Current density $\boldsymbol{J}$ is given by Ohm's law as:

$$\boldsymbol{J} = \sigma(\boldsymbol{E} + \boldsymbol{V}\times\boldsymbol{B}), \tag{1.10}$$

where σ is electrical consucivity and $\boldsymbol{E}$ is the electrical field which is assumed to be negligible here. Thus Eq. (1.10) can be rewritten as:

$$\boldsymbol{J}\times\boldsymbol{B} = (-\sigma B^2 u, 0, 0). \tag{1.11}$$

In components form, Eq. (1.8) can be expressed as:

$$\frac{\partial u}{\partial x} + \frac{\partial v}{\partial y} + \frac{\partial w}{\partial z} = 0. \tag{1.12}$$

For Maxwell fluid, $\boldsymbol{S}$ obeys the following relationship:

$$\boldsymbol{S} + \lambda_1 \frac{D\boldsymbol{S}}{Dt} = \mu\boldsymbol{A_1}, \tag{1.13}$$

where λ_1 is fluid relaxation time, D/Dt is convected time derivative and $\boldsymbol{A_1}$ is the first *Rivlin-Erickson* tensor defined as:

$$\boldsymbol{A_1} = (\boldsymbol{\nabla V}) + (\boldsymbol{\nabla V})^t = \begin{bmatrix} 2u_x & u_y + v_x & u_z + w_x \\ v_x + u_y & 2v_y & v_x + w_y \\ w_x + u_z & w_y + v_z & 2w_z \end{bmatrix}. \tag{1.14}$$

The upper convected derivative D/Dt for any vector $\boldsymbol{C}$ is defined as:

$$\frac{D\boldsymbol{C_i}}{Dt} = \frac{\partial C_i}{\partial t} + V_j C_{i,j} - V_{i,j} C_j. \tag{1.15}$$

Assigning the operator $\left(1 + \lambda_1 \frac{D}{Dt}\right)$ on both sides of Eq. (1.9) we get:

$$\rho\left(1 + \lambda_1 \frac{D}{Dt}\right)\left[\frac{d\boldsymbol{V}}{dt}\right] = -\left(1 + \lambda_1 \frac{D}{Dt}\right)\boldsymbol{\nabla}\mathrm{p} + \left(1 + \lambda_1 \frac{D}{Dt}\right)(\boldsymbol{\nabla}.\boldsymbol{S}) + \left(1 + \lambda_1 \frac{D}{Dt}\right)(-\sigma B^2 u, 0, 0). \tag{1.16}$$

The assumption of no modified pressure gradient leads to the following equation:

$$\rho\left(1 + \lambda_1 \frac{D}{Dt}\right)\left[\frac{d\boldsymbol{V}}{dt}\right] = \boldsymbol{\nabla}.\left(1 + \lambda_1 \frac{D}{Dt}\right)\boldsymbol{S} + \left(1 + \lambda_1 \frac{D}{Dt}\right)(-\sigma B^2 u, 0, 0). \tag{1.17}$$

Utilizing Eq. (1.13), Eq. (1.17) can be rewritten as:

$$\rho\left(1 + \lambda_1 \frac{D}{Dt}\right)\left[\frac{d\boldsymbol{V}}{dt}\right] = \mu(\boldsymbol{\nabla}.\mathbf{A_1}) + \left(1 + \lambda_1 \frac{D}{Dt}\right)(-\sigma B^2 u, 0, 0). \tag{1.18}$$

Using definitions given in (1.14) and (1.15), Eq. (1.18) in the $x-$ and $y-$ components, we get the following momentum equations for Maxwell fluid:

$$u\frac{\partial u}{\partial x} + v\frac{\partial u}{\partial y} + w\frac{\partial u}{\partial z} + \lambda_1 \begin{bmatrix} u^2\frac{\partial^2 u}{\partial x^2} + v^2\frac{\partial^2 u}{\partial y^2} + w^2\frac{\partial^2 u}{\partial z^2} \\ +2uv\frac{\partial^2 u}{\partial x \partial y} + 2vw\frac{\partial^2 u}{\partial y \partial z} + 2uw\frac{\partial^2 u}{\partial x \partial z} \end{bmatrix} = \nu\frac{\partial^2 u}{\partial z^2} - \frac{\sigma B^2}{\rho}\left(u + \lambda_1 w\frac{\partial u}{\partial z}\right), \tag{1.19}$$

$$u\frac{\partial v}{\partial x} + v\frac{\partial v}{\partial y} + w\frac{\partial v}{\partial z} + \lambda_1 \begin{bmatrix} u^2\frac{\partial^2 v}{\partial x^2} + v^2\frac{\partial^2 v}{\partial y^2} + w^2\frac{\partial^2 v}{\partial z^2} \\ +2uv\frac{\partial^2 v}{\partial x \partial y} + 2vw\frac{\partial^2 v}{\partial y \partial z} + 2uw\frac{\partial^2 v}{\partial x \partial z} \end{bmatrix} = \nu\frac{\partial^2 v}{\partial z^2} - \frac{\sigma B^2}{\rho}\left(v + \lambda_1 w\frac{\partial v}{\partial z}\right). \tag{1.120}$$

1.3.3 Thermal conductivity

The intrinsic property of a material which explains the materials capability to conduct heat is known as thermal conductivity. Its S.I unit is watts per meter-kelvin $(W/(m.K))$.

1.3.4 Electrical conductivity

It is defined as the ability of a material to allow the flow of electric current. Mathematically:

$$\sigma = \frac{l}{RA}, \tag{1.21}$$

where l represents length of the material, R gives resistance of the material and A gives area of the material. The S.I unit of σ is siemens per meter (Sm^{-1}).

1.3.5 $bvp4c$

Flows occurring in physical world are governed by complex non-linear partial differential equations. These equations may have no solution, or may have a finite number, or may have infinitely many solutions. In order to get a solution MATLAB programs require the user to provide with the initial guesses for the solution required and also for the parameters involved in the governing equations. MATLAB built in package $bvp4c$, which implements collocation method, is capable of solving a nonlinear multipoint boundary value problem. In order to utilize this technique, the third order equations are reduced to first order ordinary differential equations. The guesses are provided for more accurate results. Changes can be made in step size to increase accuracy. To get more detailed understanding of this technique Refs. [38] and [39] can be consulted.

Chapter 2

Numerical study for Sakiadis flow of Maxwell fluid with variable thermal conductivity

Fluid flow triggered by the plane surface moving with constant velocity in an otherwise calm Maxwell fluid is revisited here. Heat transfer process accompanied by variable thermal conductivity and convective boundary is considered. It is assumed that thermal conductivity exhibits a directly linear temperature dependency and such assumption makes the convective condition nonlinear in temperature. Flow field is exposed to vertical magnetic field with flux density B. A reliable and easy to implement numerical procedure is invoked to retrieve velocity and temperature functions. Emphasis is paid towards the effects of rheology (viscoelasticity) and variable thermal conductivity on the flow model.

.

2.1 Problem formulation

The problem under consideration involves a steady and laminar Maxwell fluid flow resulting by motion of a flat plate with constant velocity U. Heat transfer mechanism is induced by providing convection at the plate with temperature T_f and heat transfer coefficient h_f, whereas T_∞ denotes the free stream temperature such that $T_f > T_\infty$. The system is permeated to vertical magnetic field with flux density B. Electric field is ignored whereas induced magnetic field becomes negligible by considering small magnetic Reynolds number. The Lorentz force vector takes the form $\overrightarrow{F_B} = (-\sigma B^2 u, 0,0)$. The physical sketch of the model is given by Fig. 2.1. Boundary layer equations embodying the problem under discussion are:

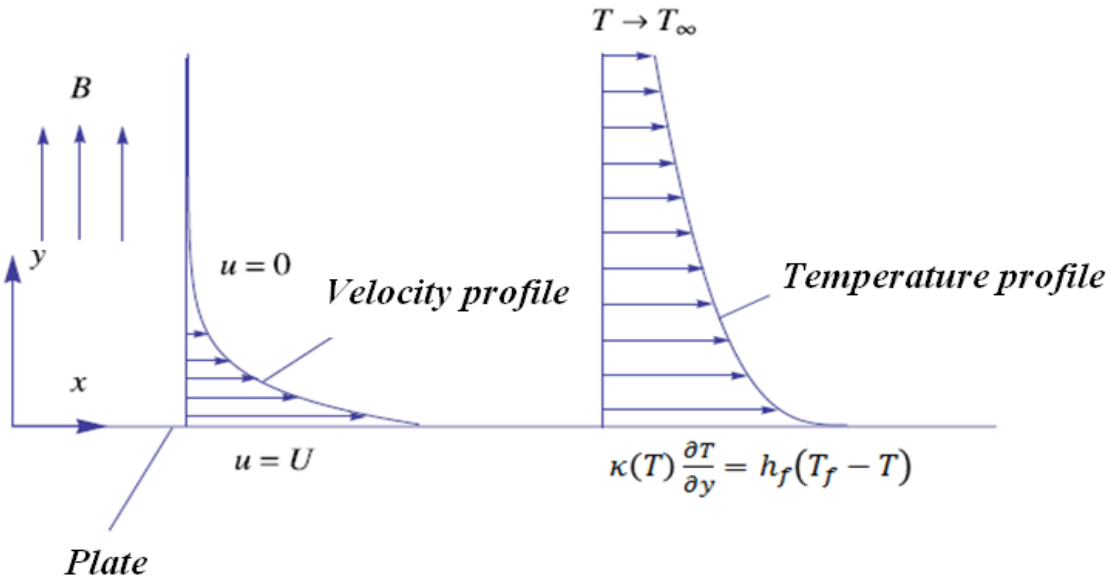

Fig 2.1: Physical sketch of the problem

$$\frac{\partial u}{\partial x} + \frac{\partial v}{\partial y} = 0, \tag{2.1}$$

$$u\frac{\partial u}{\partial x} + v\frac{\partial u}{\partial y} + \lambda_1\left(u^2\frac{\partial^2 u}{\partial x^2} + v^2\frac{\partial^2 u}{\partial y^2} + 2uv\frac{\partial^2 u}{\partial x \partial y}\right) = \nu\frac{\partial^2 u}{\partial y^2} - \frac{\sigma B^2}{\rho}\left(u + \lambda_1 v\frac{\partial u}{\partial y}\right), \tag{2.2}$$

$$\rho c_p\left(u\frac{\partial T}{\partial x} + v\frac{\partial T}{\partial y}\right) = \frac{\partial}{\partial y}\left(\kappa(T)\frac{\partial T}{\partial y}\right). \tag{2.3}$$

The assumptions of no slip and convective heating at the wall produce the following conditions:

$$u = U,\ v = 0, -\kappa(T)\frac{\partial T}{\partial y} = h_f(T_f - T) \quad \text{at} \quad y = 0, \tag{2.4a}$$

and following holds at the ambient:

$$u \to 0, \qquad T \to T_\infty \quad \text{as} \quad y \to \infty, \tag{2.4b}$$

where (u, v) represent velocities in the (x, y) directions respectively. λ_1 is termed fluid relaxation time, ν symbolizes kinematic viscosity, ρ represents density, $h_f = h/\sqrt{x}$ is the heat transfer coefficient, T is local fluid temperature, c_p shows the specific heat capacity and $\kappa(T)$ stands for thermal conductivity which has the following form:

$$\kappa(T) = \kappa_\infty \left(1 + \epsilon \frac{T - T_\infty}{T_f - T_\infty}\right). \tag{2.5}$$

In Eq. (2.5), $\epsilon > 0$ is constant and κ_∞ is the thermal conductivity of the ambient fluid.

In [40], it was shown that problem is reducible to a locally similar system by substituting:

$$\eta = \sqrt{\frac{U}{\nu x}}\, y, \quad u = U f', \quad v = -\frac{1}{2}\sqrt{\frac{\nu U}{x}}\,(f - \eta f'), \quad \theta(\eta) = \left(\frac{T - T_\infty}{T_f - T_\infty}\right), \tag{2.6}$$

where $f(\eta)$ represents dimensionless stream function and $\theta(\eta)$ gives non-dimensional temperature. The continuity equation, Eq. (2.1) is by design satisfied whereas Eq. (2.2), Eq. (2.3) and boundary conditions given by Eqs. (2.4a and 2.4b) become:

$$f''' + \frac{1}{2} f f'' - \frac{De}{2}(2 f f' f'' + \eta f'^2 f'' + f^2 f''') - M^2(f' - De(f - \eta f') f'') = 0, \tag{2.7}$$

$$(1 + \epsilon\theta)\theta'' + \epsilon\theta'^2 + \frac{Pr}{2}\, f\theta' = 0, \tag{2.8}$$

$$f(0) = 0, \qquad f'(0) = 1, \qquad [1 + \epsilon\theta(0)]\theta'(0) = -Bi\big(1 - \theta(0)\big), \tag{2.9a}$$

$$f'(\infty) \to 0 \quad \theta(\infty) \to 0, \tag{2.9b}$$

where $De = \lambda_1 U/2x$ is local Deborah number, $M = \sqrt{\sigma B^2 x/\rho U}$ is magnetic interaction parameter, $Pr = \nu/\alpha$ is the Prandtl number, $Bi = h/k_\infty\sqrt{\nu/U}$ is the Biot number.

Local Nusselt number Nu_x is used in calculations of heat transfer between a moving fluid and a solid body, a physical quantity of great importance, is defined as:

$$Nu_x = \frac{x q_w}{\kappa(T)\big(T_f - T_\infty\big)}, \tag{2.10}$$

where $q_w = -\kappa(T)(\partial T/\partial y)_{y=0}$is the wall heat flux. Using (2.6) and substituting q_w in Eq. (2.10) we get:

$$Re_x{}^{-1/2}\, Nu_x = -\theta'(0), \tag{2.11}$$

where $Re_x = xU/\nu$ represents local Reynolds number.

2.2 Numerical method

The boundary value problem (bvp) stated by Eqs. (2.7) and (2.8) with conditions (2.9a) and (2.9b) is solved using MATLAB package bvp4c. Let us substitute,

$$f' = p,\ \ p' = q,\ \ \theta' = z, \tag{2.12}$$

in Eqs. (2.7) and (2.8), we obtain:

$$q' = \left\{-\frac{1}{2}fq + \frac{De}{2}(2fpq + \eta p^2 q) + M^2(p - De(f - \eta p)q)\right\} / \left(1 - \frac{De}{2}f^2\right), \tag{2.13}$$

$$z' = -\left\{\epsilon z^2 + \frac{Pr}{2}fz\right\} / (1 + \epsilon\theta). \tag{2.14}$$

Eqs. (2.13) and (2.14) are written in bvp4c code along with the conditions (2.9a) and (2.9b). We initiate the computations by initially choosing low η_∞. The computations are performed at different η_∞'s (say 10, 11, 12, 13 etc.) until the initial slopes $f''(0)$ and $\theta'(0)$ become consistent and residuals of far field conditions stay less than 10^{-6}.

2.3 Numerical results and discussion

To ascertain that computations are accurate, the results of $-\theta'(0)$ are compared in Table 2.1 with previous works of Cortell [41] and Mustafa et al. [40] and such comparison appears convincing. Having the accuracy of our code being established, we will now discuss the new findings of our analysis and discuss how temperature dependent thermal conductivity impacts our flow model. In Table 2.2, numerical data of local Nusselt number represented by $-\theta'(0)$ is compared by varying embedded parameters. It is detected that by increasing De or Pr, $-\theta'(0)$ increases in absolute sense. However, a decreasing trend in local Nusselt number is found for growing values of M and ϵ. This is because variable thermal conductivity depends upon ϵ, and since epsilon increases, thermal conductivity increases which results in rise of temperature which consequently leads to lower temperature gradient.

Table 2.1: Comparison with local Nusselt number $-\theta'(0)$ obtained by Cortell [41] and Mustafa et al. [40] when $De = M = \epsilon = 0$ and $Bi = 1000000$:

Pr	$-\theta'(0)$		
	Cortell [41]	Mustafa et al. [40]	Present
0.6	0.313519	0.31352	0.313519
5.5	1.216049	1.21605	1.216057
7	1.387033	1.38703	1.387038
10	1.680293	1.68029	1.680297
50	3.890918	3.89091	3.890929
100	5.544663	5.54464	5.544655

In Fig. 2.2**,** when the flow is not exposed to magnetic field, a cross over in $u-$ velocity curves is noticed indicating that velocity increases near the plate and decreases far from it when *De* becomes large. This mixed behavior is not seen by inducing transverse magnetic field to the flow. Velocity as well as boundary layer thickness is inversely related to the local Deborah number. Furthermore, boundary layer thickness is much suppressed by the action of magnetic field. However, Fig. 2.3 illustrates that heat penetration depth progresses as magnetic flux density enlarges. The striking influence of rheology is the enhancement of thermal boundary layer thickness for increasing values of *De*. In Fig. 2.4, variation in temperature profile by changing Prandtl number is observed. Large Prandtl number Pr indicates relatively lower thermal conductivity at the ambient. Hence increasing Pr is expected to shorten heat penetration depth. Fig. 2.5 illustrates the behavior of convective boundary on the temperature θ. Higher values of Bi imply larger surface temperature which in turn produces higher penetration depth. In Fig. 2.6, when $M = 0$, local Nusselt number has a linear relationship with Deborah number. It increases (in absolute sense) for increasing Deborah number. However, opposite relationship holds when magnetic force is brought into effect. To understand the significance of parameter ϵ with regards to heat transfer, Fig. 2.7 is obtained. A marked reduction in $|\theta'(0)|$ is seen for higher values of ϵ. This concludes that the consideration of constant thermal conductivity (in practical processes) may lead to overestimates of local Nusselt number. In Fig. 2.8, when we

increase Biot number, it results in increase in local Nusselt number. When Bi approaches ∞ local Nusselt number becomes constant.

Table 2.2: Computational results of local Nusselt number for various values of $De, M, \Pr$ and ϵ with $Bi = 0.5$.

De	M	Pr	ϵ	$-\theta'(0)$
0	0	3	0	0.31696815
			0.5	0.27386683
			1	0.24302909
		7	0	0.36751738
			0.5	0.32871833
			1	0.29895069
	1	3	0	0.29705083
			0.5	0.25242898
			1	0.22112219
		7	0	0.357126
			0.5	0.31669739
			1	0.28606194
1	0	3	0	0.31890243
			0.5	0.27656686
			1	0.24644296
		7	0	0.36919746
			0.5	0.331166
			1	0.30210732
	1	3	0	0.29261641
			0.5	0.24751319
			1	0.21594574
		7	0	0.35577038
			0.5	0.31508706
			1	0.28428662

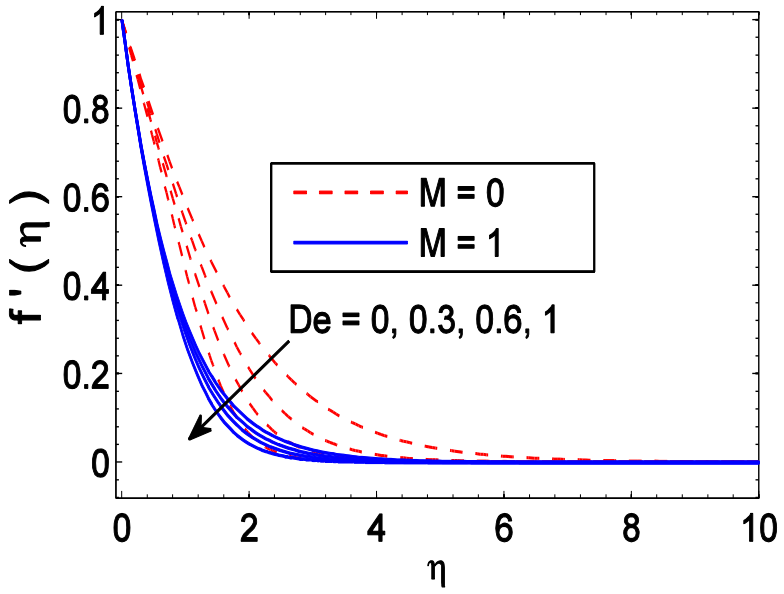

Fig. 2.2: Variation in velocity curve f' with η for different Deborah numbers.

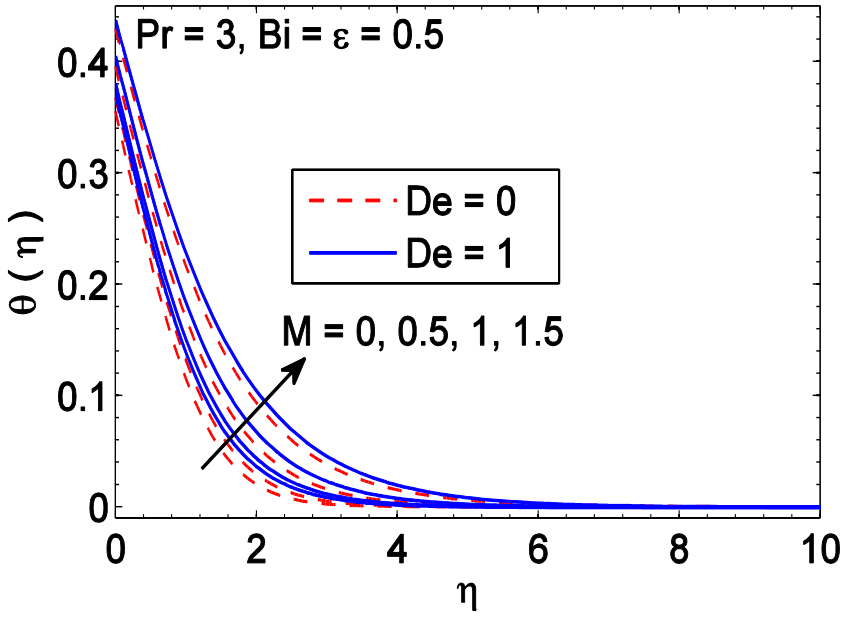

Fig. 2.3: Variation in temperature curve θ with η for different magnetic field parameters.

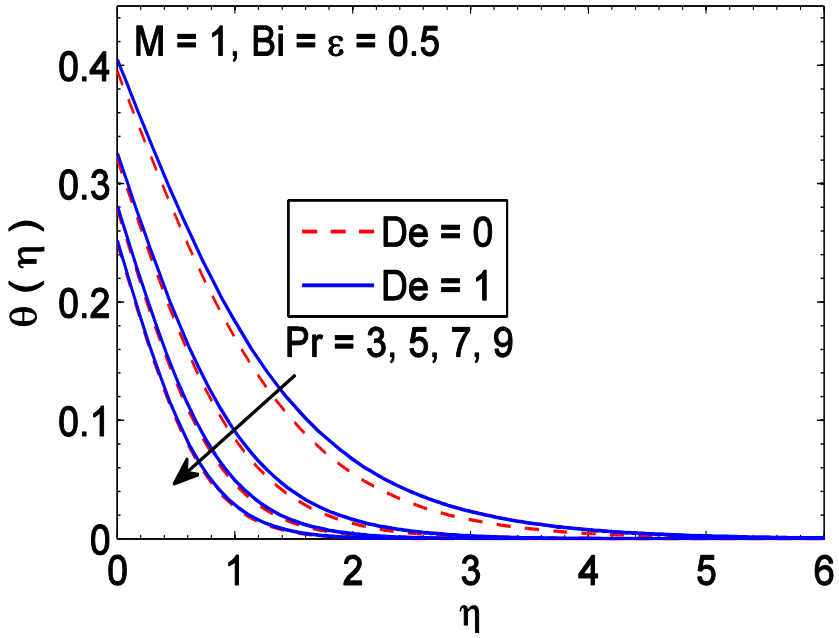

Fig. 2.4: Variation in temperature curve θ with η for different Prandtl numbers.

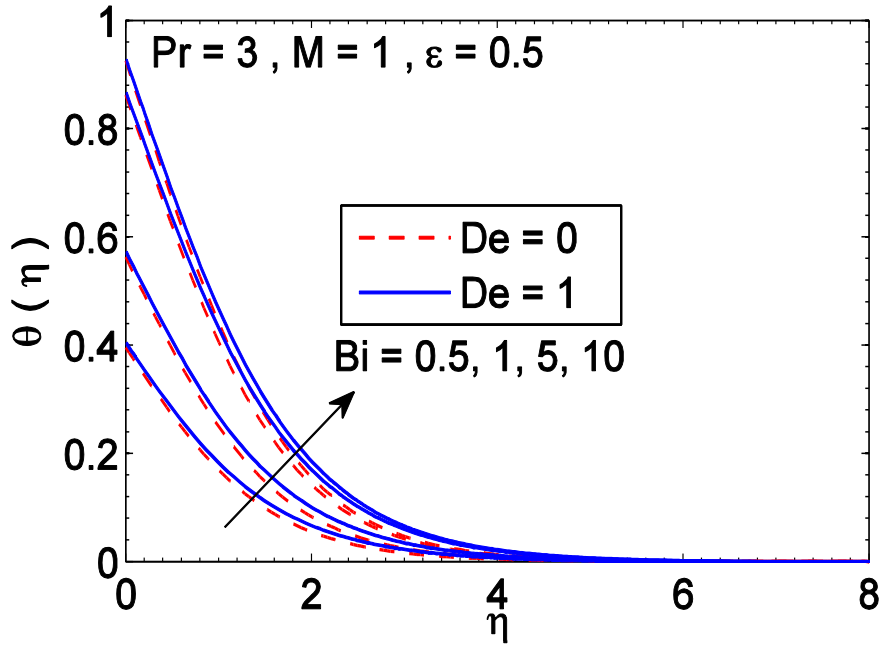

Fig. 2.5: Variation in temperature curve θ with η for different Biot numbers.

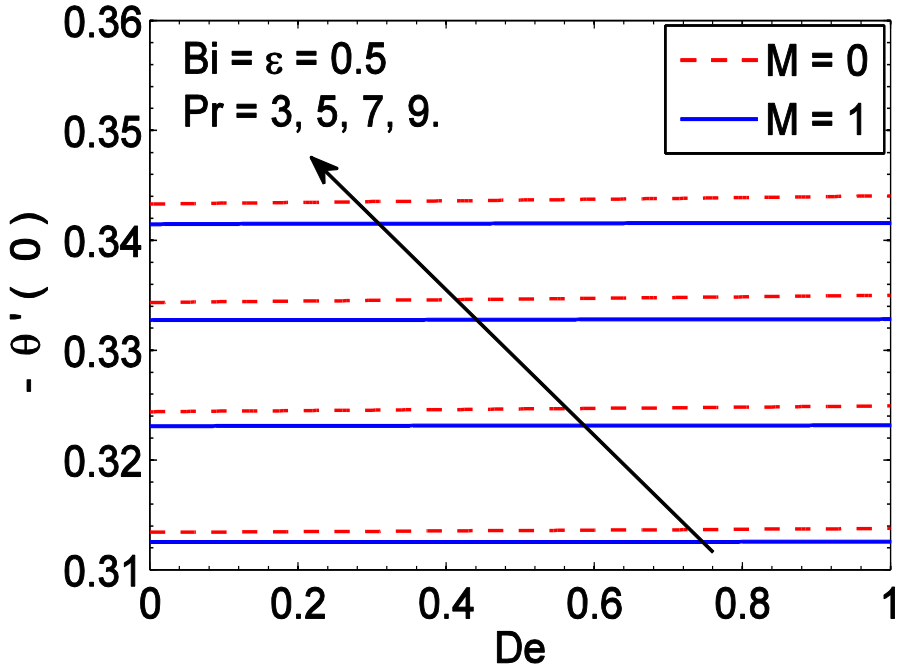

Fig. 2.6: Variation in local Nusselt number $-\theta'(0)$ with De for different Prandtl numbers

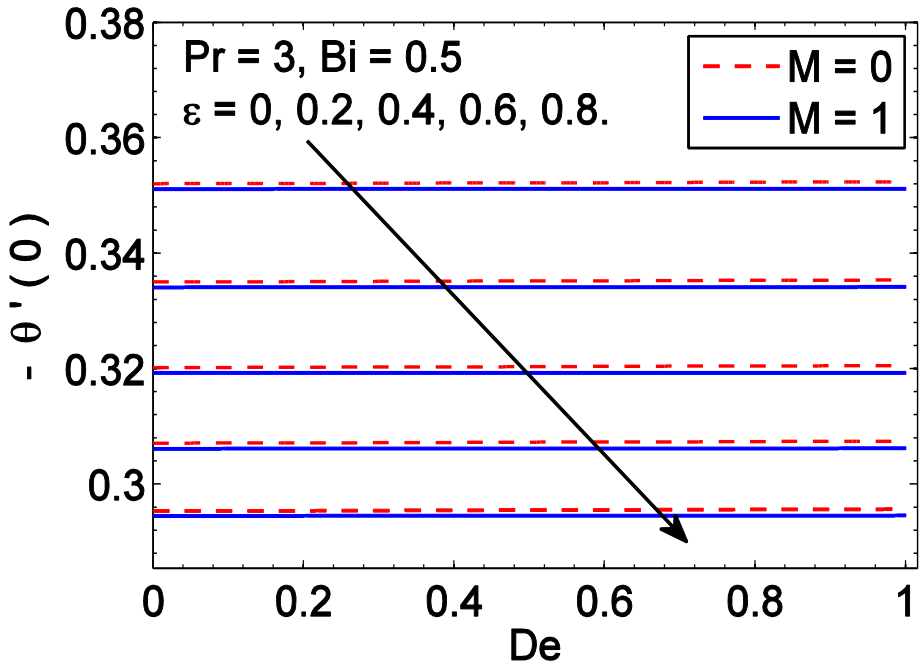

Fig. 2.7: Variation in local Nusselt number $-\theta'(0)$ with De for different values of parameter ϵ.

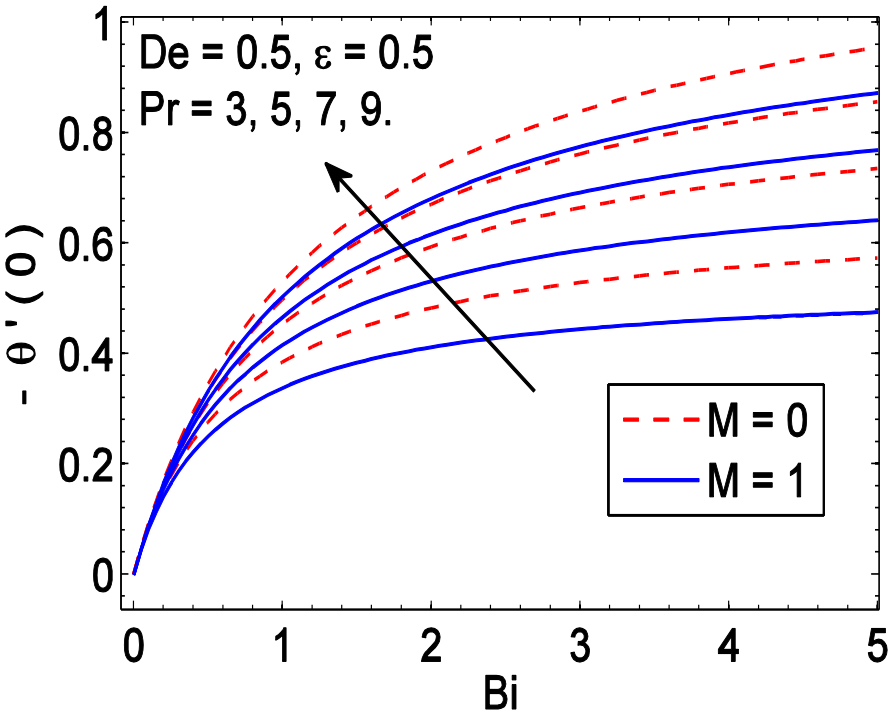

Fig. 2.8: Variation in local Nusselt number $-\theta'(0)$ with Bi for different Prandtl numbers.

2.4 Concluding remarks

Analysis of MHD Sakiadis flow of Maxwell fluid influenced by temperature dependent thermal conductivity is theoretical focus of this chapter. The conclusions drawn from the present study are in excellent agreement to those from recent bibliography. Listed below are the key findings reached from numerical treatment of the governing model:

• In the absence of magnetic field ($M = 0$), velocity increases near the plate and decreases just away from it with an increase in Deborah number.

• Velocity of fluid as well as momentum boundary layer thickness decreases with the increase in either Deborah number or magnetic field parameter.

• The increase in thermal conductivity parameter raises the temperature of the fluid across the boundary layer. This again increases the thickness of boundary layer.

• Local Nusselt number is proportional to the local Deborah number. The trend is reversed when magnetic field is brought into effect.

• Increase in Biot number causes increase in local Nusselt number. When biot number grows sufficiently large, $-\theta'(0)$ becomes nearly constant.

Chapter 3

Numerical study for Sakiadis flow of MHD Maxwell fluid inspired by nonlinear radiation heat flux

This chapter is motivated to formulate fluid flow around a moving porous plate immersed in a viscoelastic fluid subjected to thermal radiation effects. Thermal process is characterized by implementing convective boundary heating. A locally similar treatment is pursued to resolve flow and heat transfer problems. The first section formulates governing problem under boundary layer approximations. Numerical calculations signifying the consequences of nonlinear radiation on the flow model are deliberated in section 3.3. Section 3.4 outlines the important findings of this research.

3.1 Problem formulation

The considered plate within this research rests in the plane $y = 0$ where heat source of volumetric heat generation $Q^* = Q/x$ is present. Heat transfer occurs as a result of heating of the absorbing fluid and plate by radiation. The flow is triggered by the motion of plate in the positive $x-$direction with constant velocity U**.** The plate is assumed porous with wall suction velocity $v_w > 0$. Temperature at the boundary is passively maintained by convective heating with temperature T_f. T_∞ shows temperature at the far field such that $T_f > T_\infty$. The field flow is exposed to vertical magnetic field with uniform magnetic flux density B. Accounting these assumptions, the conservation equations can be casted in the following forms:

$$\frac{\partial u}{\partial x} + \frac{\partial v}{\partial y} = 0, \tag{3.1}$$

$$u\frac{\partial u}{\partial x} + v\frac{\partial u}{\partial y} + \lambda_1\left(u^2\frac{\partial^2 u}{\partial x^2} + v^2\frac{\partial^2 u}{\partial y^2} + 2uv\frac{\partial^2 u}{\partial x \partial y}\right) = \nu\frac{\partial^2 u}{\partial y^2} - \frac{\sigma B^2}{\rho}\left(u + \lambda_1 v\frac{\partial u}{\partial y}\right), \tag{3.2}$$

$$u\frac{\partial T}{\partial x} + v\frac{\partial T}{\partial y} = \alpha\frac{\partial^2 T}{\partial y^2} - \frac{1}{\rho C_p}\frac{\partial q_r}{\partial y} + \frac{Q^*}{\rho c_p}(T - T_\infty), \tag{3.3}$$

with the conditions,

$$u = U,\ \ v = -v_w = -v_0 x^{-1/2}\ , -\kappa\ \frac{\partial T}{\partial y} = h_f\big(T_f\ -\ T\big)\quad \text{at}\ \ y = 0, \tag{3.4a}$$

and following holds at the ambient:

$$u\ \to 0, \qquad T\ \to T_\infty\quad \text{as}\quad y\ \to \infty. \tag{3.4b}$$

In Eqs. (3.1) - (3.4), (u, v) denote the horizontal and vertical velocities, λ_1 stands for fluid relaxation time, α symbolizes thermal diffusivity, ρ stands for density, the symbol c_p represents specific heat capacity, $h_f = h\, x^{-1/2}$ with $h > 0$ is heat transfer coefficient of the (convective) fluid and q_r measures heat flux due to radiation.

For optically thick media, Rosseland [42] proposed following approximation of heat flux q_r:

$$q_r = -\Big(\frac{4\sigma_{SB}}{3a_R}\Big)\frac{\partial T^4}{\partial y}, \tag{3.5}$$

where $a_R(m^{-1})$ is referred as mean-absorption coefficient and $\sigma_{SB} = 5.6697 \times 10^{-8} Wm^{-2}K^{-4}$ symbolizes Stefan-Boltzman constant.

For linearization of heat flux given by Eq. (3.5), we write Taylor series of T^4 about T_∞ and subsequently neglect the square and higher powers involving $(T - T_\infty)$ by considering small temperature gradients. That is,

$$T^4 \cong 4T{T_\infty}^3 - 3T_\infty^4. \tag{3.6}$$

The energy equation Eq. (3.3) for the linear thermal radiation case will then become:

$$u\frac{\partial T}{\partial x}\ + v\frac{\partial T}{\partial y} = \frac{\partial}{\partial y}\left[\left(\alpha + \frac{16\sigma_{SB}{T_\infty}^3}{3a_R(\rho c_p)}\right)\frac{\partial T}{\partial y}\right] + \frac{Q^*}{\rho C_p}(T\ -\ T_\infty). \tag{3.7}$$

Whereas, for the nonlinear case, inserting Eq. (3.5) into Eq. (3.3) brings the following energy equation in temperature T:

$$u\frac{\partial T}{\partial x}\ + v\frac{\partial T}{\partial y} = \frac{\partial}{\partial y}\left[\left(\alpha + \frac{16\sigma_{SB}T^3}{3a_R(\rho c_p)}\right)\frac{\partial T}{\partial y}\right] + \frac{Q^*}{\rho C_p}(T\ -\ T_\infty). \tag{3.8}$$

In [42], it was shown that problem is reducible to a locally similar system by substituting:

$$\eta = \sqrt{\frac{U}{\nu x}}\, y, \quad u = Uf', \quad v = -\frac{1}{2}\sqrt{\frac{\nu U}{x}}\,(f - \eta f'), \quad T = T_\infty\left(1 + \left(\theta_f - 1\right)\theta\,(\eta)\right), \tag{3.9}$$

where $\theta_f = T_f/T_\infty (> 1)$ is termed temperature ratio parameter and η is local similarity variable.

In view of Eq. (3.9), the mass-conservation equation is identically fulfilled, while Eq. (3.2) and Eq. (3.8) are transformed to the following ODEs:

$$f''' + \frac{1}{2}ff'' - \frac{De}{2}(2ff'f'' + \eta f'^2 f'' + f^2 f''') - M^2(f' - De(f - \eta f')f'') = 0, \tag{3.10}$$

$$\frac{Pr}{2}f\theta' + S\theta + \left[\theta'\left(1 + \frac{4}{3}Rd\left(1 + \left(\theta_f - 1\right)\theta\right)^3\right)\right]' = 0. \tag{3.11}$$

Here $De = \lambda_1 U/2x$ is termed local Deborah number, $M = (\sigma B^2 x/\rho U)^{1/2}$ is referred as magnetic interaction parameter, $Pr = \nu/\alpha$ denotes the Prandtl number, $S = Q\nu/\kappa U$ stands for heat generation parameter, Rd represents thermal radiation parameter.

The boundary conditions in Eqs. (3.4a) and (3.4b) are transformed as follows:

$$f(0) = A, \qquad f'(0) = 1, \qquad \theta'(0) = -Bi\left(1 - \theta(0)\right), \tag{3.12a}$$

$$f'(\infty) \to 0 \quad \theta(\infty) \to 0, \tag{3.12b}$$

where $A = 2v_0/\sqrt{\nu U}$ (> 0) is suction strength parameter, and $Bi = h/k(\nu/U)^{1/2}$ represents Biot number.

Local Nusselt number Nu_x in this case is defined as:

$$Nu_x = \frac{xq_w}{k\left(T_f - T_\infty\right)}, \tag{3.13}$$

where $q_w = -k(\partial T/\partial y)_{y=0} + (q_r)_{y=0}$ is the wall heat flux. Using (3.7) and substituting q_w in (3.13) we get:

$$Re_x^{-1/2}\, Nu_x = -\left(1 + \frac{4}{3}Rd\left(1 + \left(\theta_f - 1\right)\theta(0)\right)^3\right)\theta'(0), \tag{3.14}$$

where $Re_x = xU/\nu$ is the local Reynolds number.

3.2 Numerical method

In order to treat the system comprising of Eqs. (3.10) and (3.11), together with conditions (3.12a) and (3.12b) and to obtain the locally similar solutions formed for heat transfer in Sakiadis flow of viscoelastic Maxwell fluid with wall suction and thermal radiation effects, MATLABs package $bvp4c$ based on collocation method is adopted. For this purpose, we use substitutions (2.12). The equivalent first-order system is given below:

$$q' = \left\{-\frac{1}{2}fq + \frac{De}{2}(2fpq + \eta p^2 q) + M^2(p - De(f - \eta p)q)\right\} / \left(1 - \frac{De}{2}f^2\right), \tag{3.15}$$

$$z' = \left\{-\frac{Pr}{2}fz - S\theta - 4Rd(\theta_f - 1)\left(1 + (\theta_f - 1)\theta\right)^2 z^2\right\} / \left(\frac{1}{1 + \frac{4}{3}Rd\left(1 + (\theta_f - 1)\theta\right)^3}\right). \tag{3.16}$$

Eqs. (3.15) and (3.16) with conditions (3.12a) and (3.12b) are treated using the approach already explained in Chapter 2.

3.3 Results and discussion

Before analyzing the results, it is worthwhile to validate the solutions obtained. The numerical data of $-\theta'(0)$ appears consistent with the previous works of Cortell [43] and Mustafa et al. [42] shown in table 3.1. Table 3.2 computes local Nusselt number data by varying key parameters of the problem. Heat transferred rate is lowered as radiation effect intensifies. It is further decreased as fluid is subjected to higher magnetic field strength. The striking effect of viscoelasticity appears to the improvement in heat transfer for increasing magnetic interaction parameter. Curves of u −velovity component (represented by f') are computed with regard to variation in local Deborah number (De). For low Deborah number ($De \ll 1$), the material's response is viscous-like. Whereas, material behaves like an elastic solid for high Deborah number (De>>1). By increasing De, the time needed for elastic effects to decay becomes higher than characteristic time. Consequently, boundary layer development is restricted and fluid flow slows down as De becomes higher. This reduction of f' imparts a higher value of $f''(0)$ as shown in Fig 3.1. Boundary layer shrinks further when higher magnetic field strength is employed. The resistive force produced by vertical magnetic field restricts fluid flow and enhances temperature profile.

The role of wall suction on horizontal velocity is demonstrated through Fig. 3.2. When the fluid is sucked from the plate, the boundary layer naturally thins. Since the viscous effect remains intact, horizontal velocity is maximum near the plate which is why reduction in horizontal velocity occurs. The influence that local Deborah can have on the temperature profile can be determined from Fig. 3.3. This Fig. depicts a decreasing trend in θ as relaxation time grows. However, a significant rise in fluid temperature is observed for increasing magnetic field strength. The outcomes of Fig. 3.3 suggest that viscoelasticity can provide improved heat transfer rate. Fig. 3.4 elucidates the change in temperature profile (θ) by changing Prandtl number Pr. As Pr increases, thermal diffusivity becomes weaker while momentum diffusion strengthens. Consequently, thermal penetration depth is shortened when Pr enlarges. The shorter penetration depth produces solid surface. Furthermore, the impact of viscoelasticity on temperature profile appears to diminish as Pr increases. In order to forecast the behavior of convective heating on temperature (θ), we plotted temperature θ against η for a variety of Biot numbers. The cases $Bi = 0$ and $Bi \to \infty$ represent isoflux wall and isothermal wall situations respectively. A marked rise on heat penetration depth is found for increasing Biot number. Physically, large Bi means higher surface temperature which imparts thicker penetration depth. The graphs of Fig. 3.5 are perfectly compatible with this physical penetration. In Fig. 3.6, we plot the temperature curves for sundry values of radiation parameter Rd. An increase in radiation parameter causes an increase in boundary layer thickness. Fig. 3.7 is obtained to foresee the suction effect on temperature distribution (θ). Our numerical results detected that $v-$ velocity components is proportional to the parameter A. Naturally, vertical flow is expected to accelerate as wall suction velocity increases. It means that (cold) fluid at ambient conditions is brought closer to the plate due to which thermal boundary layer shrinks. Consequently, heat transfer rate proportional to $\theta'(0)$ is much elevated when suction is brought into effect. Temperature ratio parameter $\theta_f (= T_f/T_\infty)$ is an indicator of difference between convective and ambient temperatures. In Fig. 3.8, temperature curves are obtained against η for different values of θ_f. Akin to the earlier studies, $\theta-$curve is concave up near the plate and concave down away from it when θ_f is sufficiently large. In other words, an inflection point arises in $\theta-$profile. The same is not observed in case of small temperature differences $(\theta_f \approx 1)$. Also, thermal boundary layer is seen to expand as θ_f enhances. Fig. 3.9 contains the curves of θ' versus η for large values of

$(\theta_f > 2)$. The inflection point exists in all the cases and location of inflection point shifts away from the plate for increasing values of θ_f. In Fig. 3.10, we identified the location of inflection point on temperature curve θ when $\theta_f = 4.5$.

Table 3.1: Computational results of $-\theta'(0)$ for different values of Pr when $M = De = Rd = S = A = 0$ and $Bi = 1000000$.

Pr	Cortell [41]	Mustafa et al. [40]	Present
0.6	0.313519	0.31352	0.31352
5.5	1.216049	1.21605	1.21605
7	1.387033	1.38703	1.38704
10	1.680293	1.68029	1.68029
50	3.890918	3.89091	3.89091
100	5.544663	5.54464	5.54464

Table 3.2: Numerical values of local Nusselt number for different values of De, M, Rd and θ_f when $Bi = 0.5,\ Pr = 7,\ A = 1$ and $S = 0.5$

De	M	Rd	θ_f	$-\left(1+\frac{4}{3}Rd\left(1+\left(\theta_f-1\right)\theta(0)\right)^3\right)\theta'(0)$
0	1	0.5	1.5	0.76309227
0.2				0.76264303
0.5				0.76174482
0.5	0	0.5	1.5	0.76892736
	0.5			0.76327111
	1			0.76174482
0.5	1	0.2	1.5	0.56989205
		0.7		0.89055559
		1		1.0831362
0.5	1	0.5	1	0.69247371
			1.5	0.76174482
			2	0.86136206

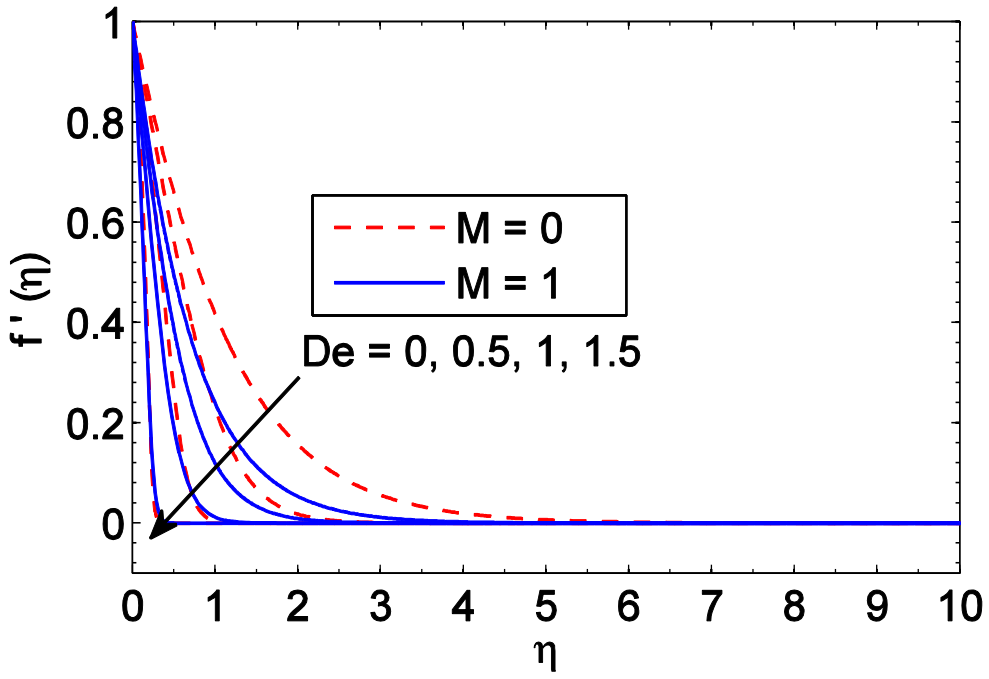

Fig. 3.1: Variation in velocity curve f' with η for different Deborah numbers.

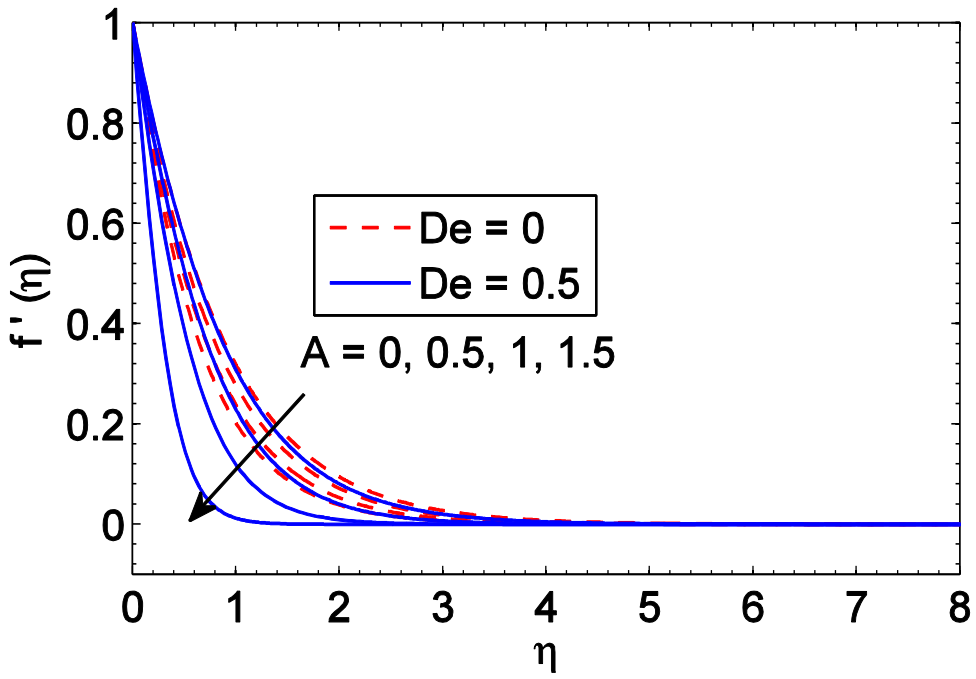

Fig. 3.2: Variation in velocity curve f' with η for different suction strength parameters.

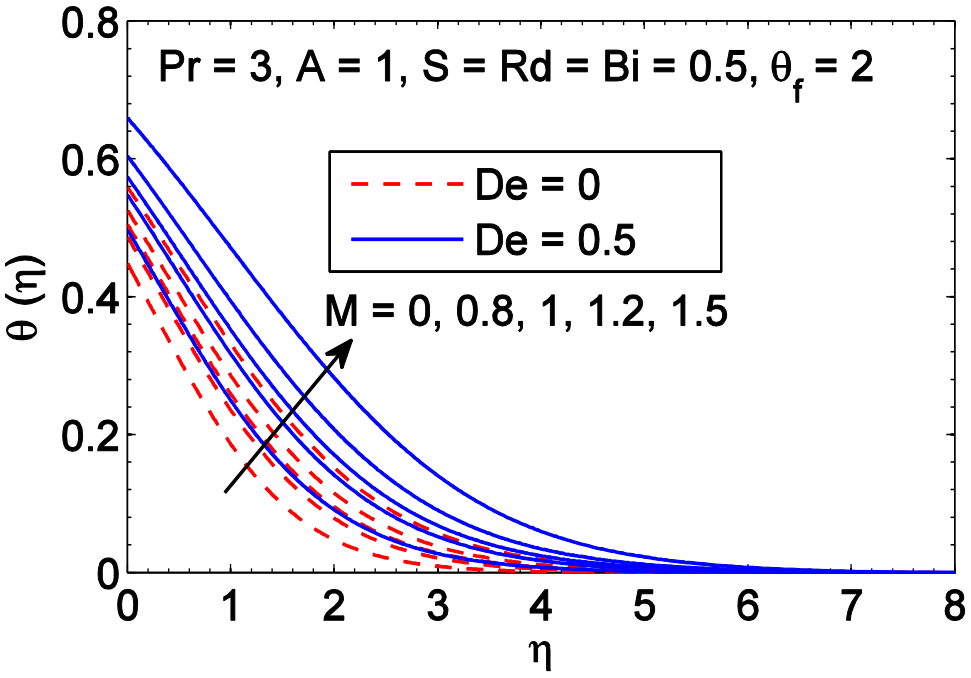

Fig. 3.3: Variation in temperature curve θ with η for different magnetic interaction parameters.

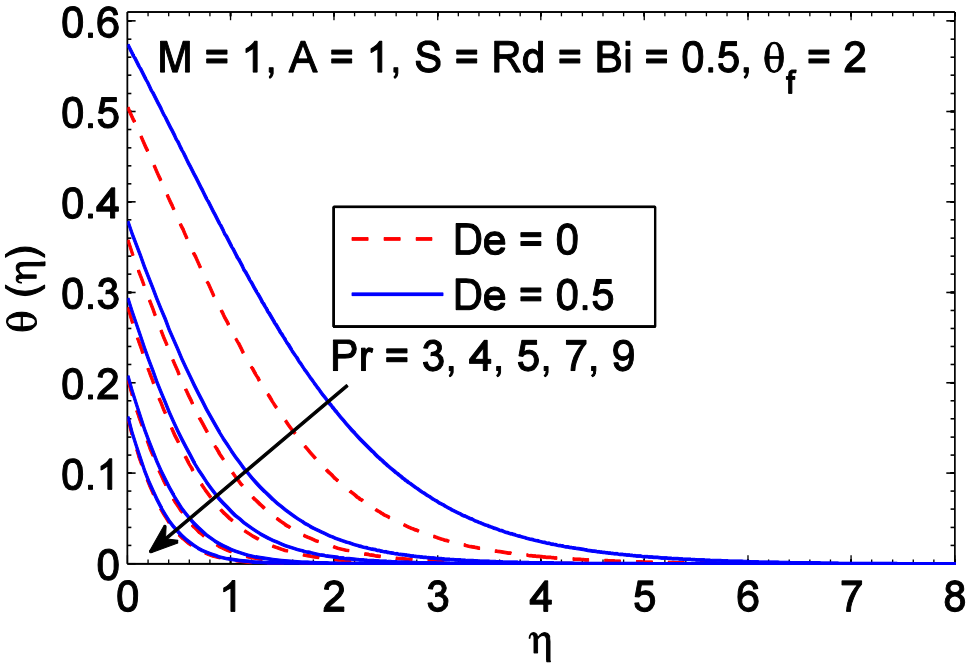

Fig. 3.4: Variation in temperature curve θ with η for different Prandtl numbers.

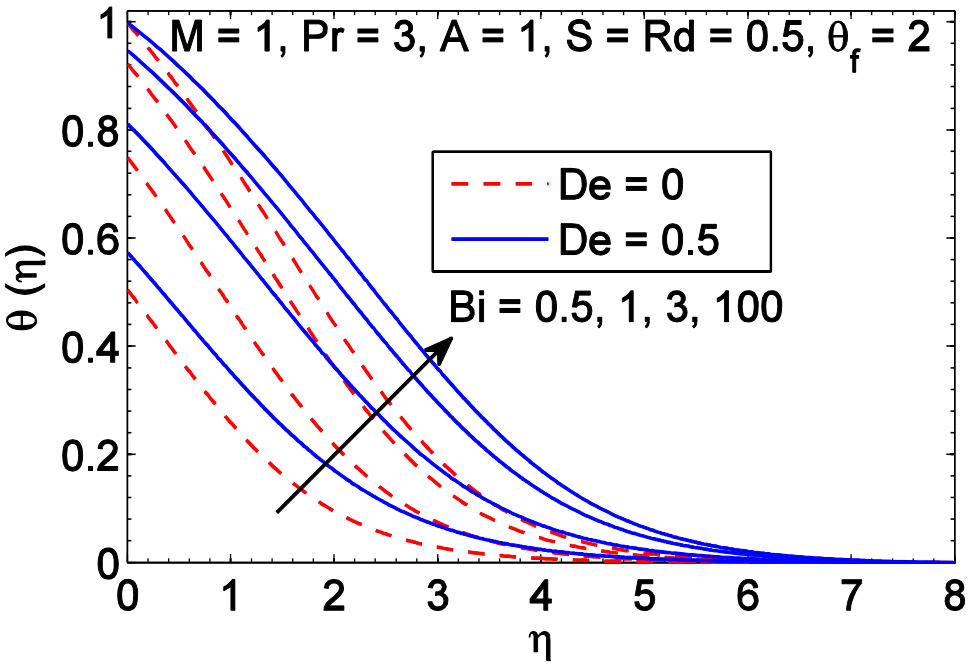

Fig. 3.5: Variation in temperature curve θ with η for different Biot numbers.

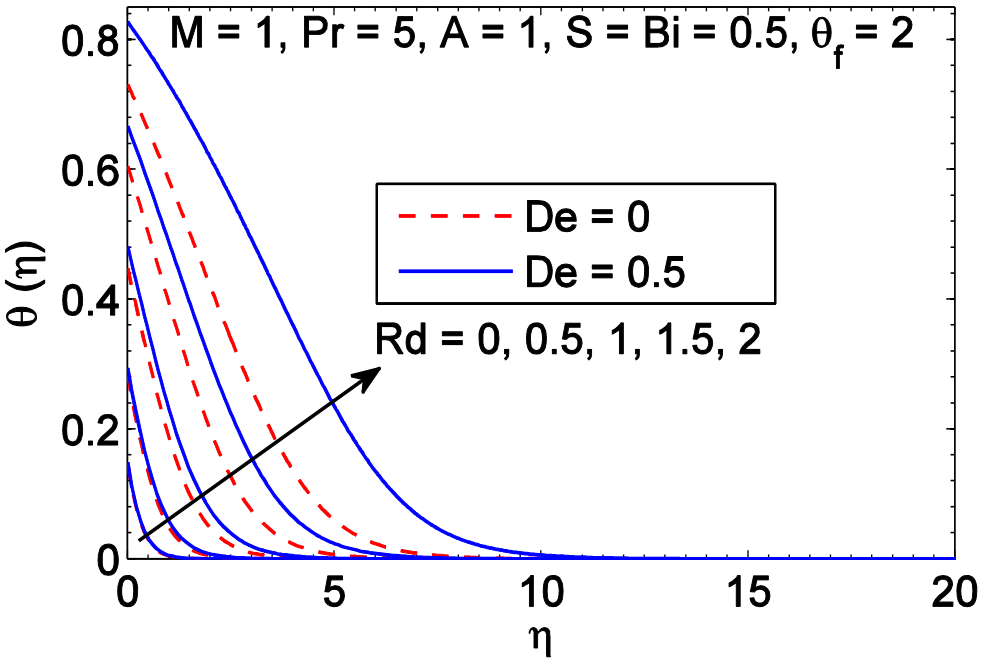

Fig. 3.6: Variation in temperature curve θ with η for different radiation parameters.

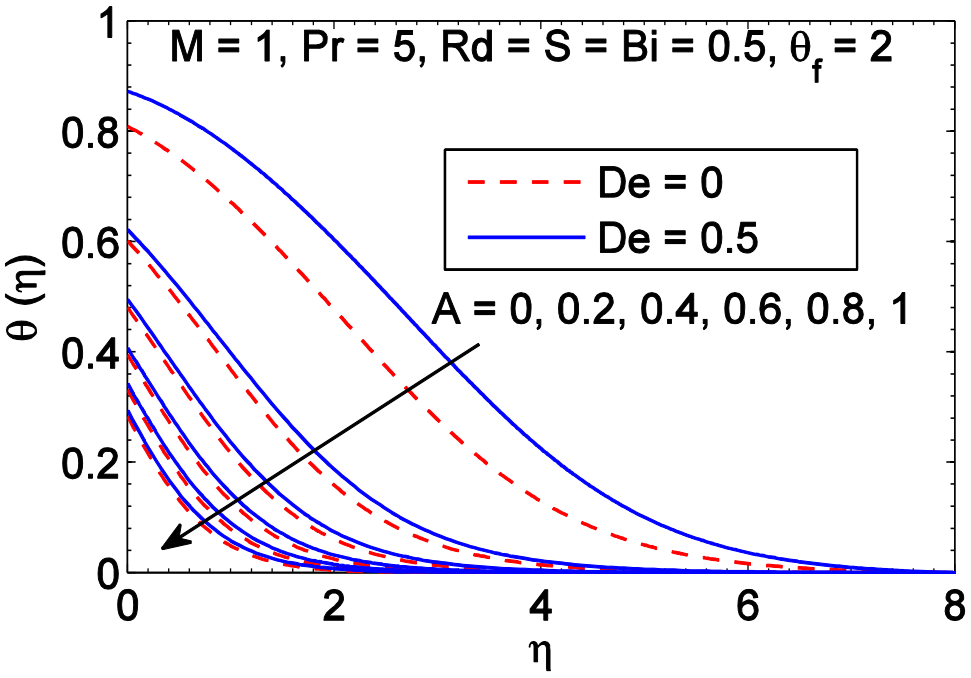

Fig. 3.7: Variation in temperature curve θ with η for different suction strength parameters.

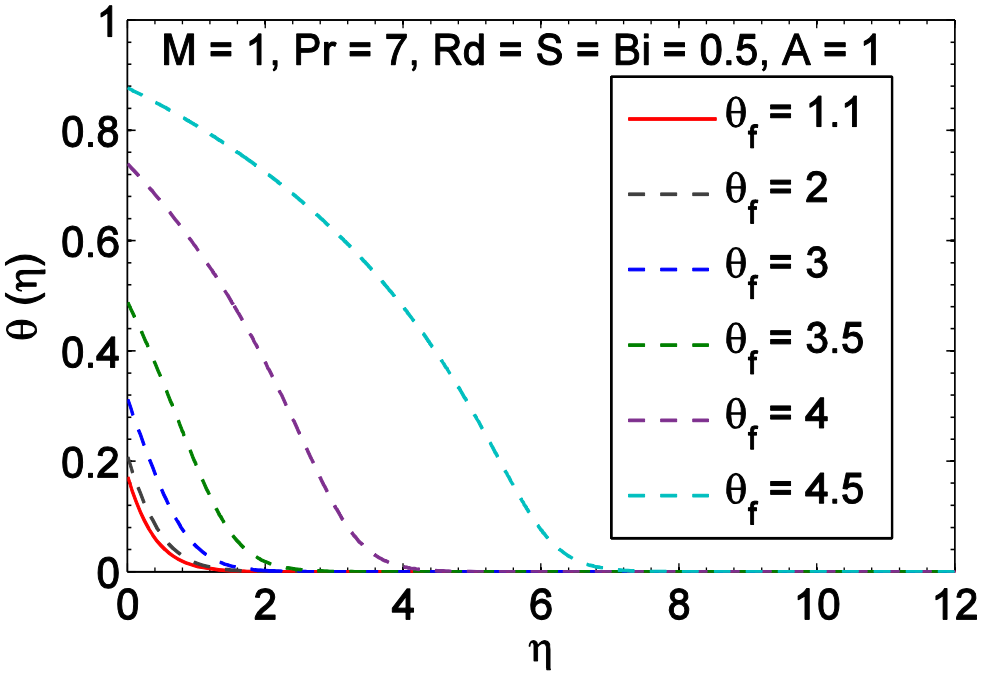

Fig. 3.8: Variation in temperature curve θ with η for different temperature ratio parameters.

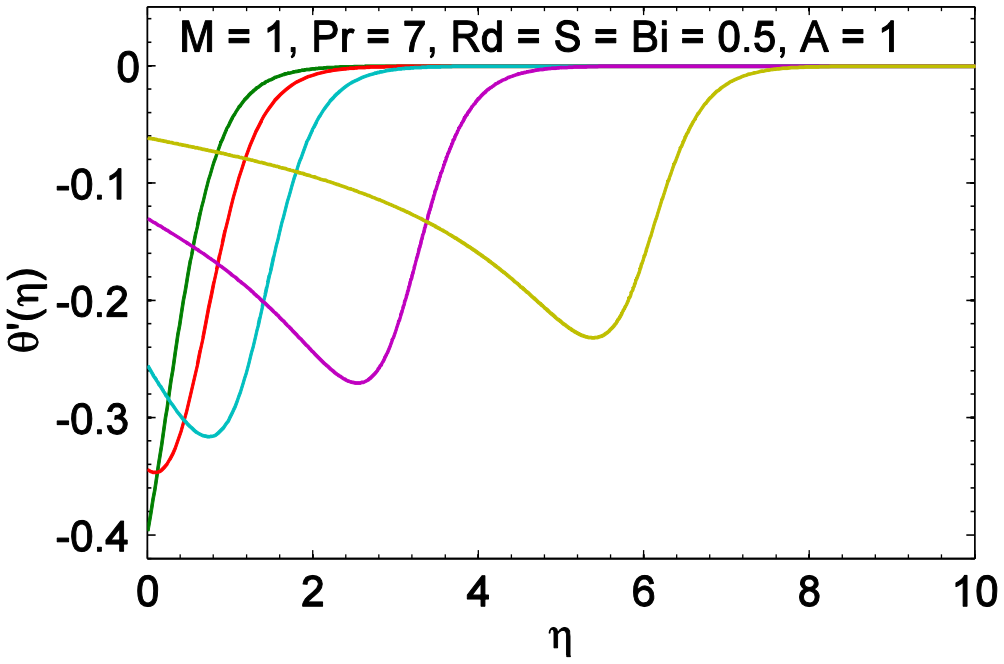

Fig. 3.9: Variation in wall temperature slope θ' for different values of temperature ratio parameter .

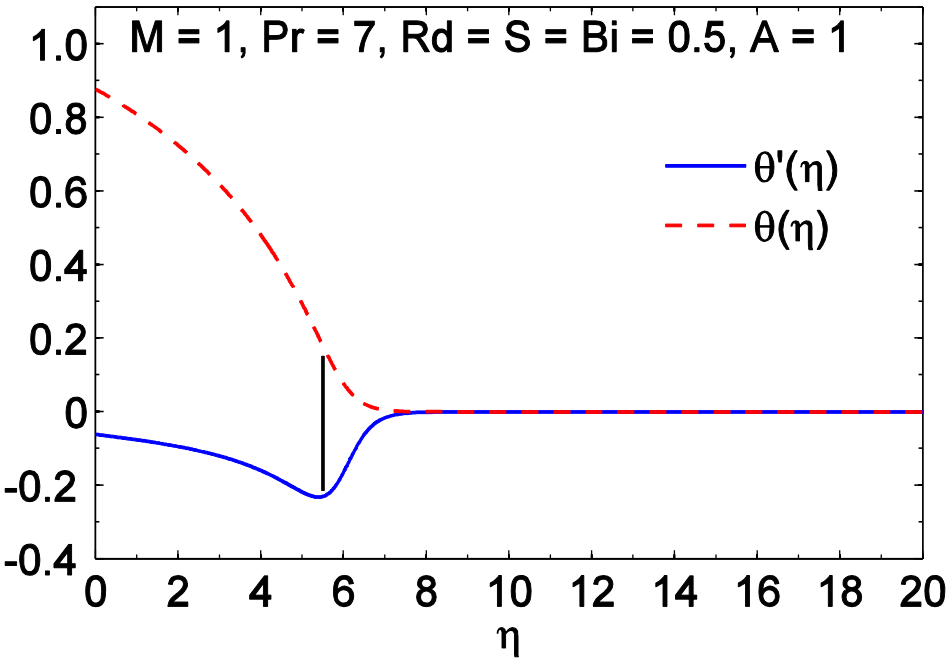

Fig. 3.10: Point of inflection for $\theta_f = 4.5$.

3.4 Concluding remarks

Analysis of MHD Sakiadis flow of viscoelastic fluid influenced by radiative heat transfer is theoretical focus of this research. The conclusions drawn from the present study are in full line with those from recent bibliography. We list below the key findings reached from numerical treatment of the governing model:

- Temperature θ has direct relationship with both fluid relaxation time and magnetic field intensity B.
- Wall suction opposes the horizontally driven flow by the plate. Naturally, suction elevates the wall skin friction as well as volumetric flow rate.
- Increasing suction drastically lowers the thermal penetration depth. This outcome signals that wall suction physically favors the heat transfer rate from the surface.
- Keeping in view the technological processes, suction appears to have definite role in improving wall cooling efficiency.
- When $\theta_f \approx 1,$ temperature curve is concave up throughout the boundary layer. However, temperature function has horizontal tangents at any point inside the boundary layer when θ_f is large.
- Wall skin friction grows and heat transfer rate is lowered when fluid is exposed to vertical magnetic field.

References

1. H. Blasius, Grenzschichten in Flussigkeiten Mit Kleiner Reibung. Z. Math. Phys. 56 (1908) 1–37.
2. B. C. Sakiadis, Boundary-layer Behaviour on Continuous Solid Surfaces; Boundarylayer Equations for 2-dimensional and Axisymmetric Flow, AIChE J. 7 (1961) 26–28.

3. B. C. Sakiadis, Boundary-layer Behaviour on Continuous Solid Surfaces; Boundarylayer Equations for 2-dimensional and Axisymmetric Flow, AIChE J. 7 (1961) 221–225
4. K. Sadeghy, A. H. Najafi, M. Saffaripour, Sakiadis flow of an upper-convected Maxwell fluid, Int. J. Non-Linear Mech. 40 (2005) 1220-1228.
5. M. Kumaria, G. Nath, Steady mixed convection stagnation-point flow of upper convected Maxwell fluids with magnetic field, Int. J. Non-Linear Mech. 44 (2009) 1048-1055.
6. T. Hayat, Z. Abbas, M. Sajid, MHD stagnation point flow of an upper-convected Maxwell fluid over a stretching surface, Chaos Solitons Fractals 39 (2007) 840-848.
7. S. Shateyi, A new numerical approach to MHD flow of a Maxwell fluid past a vertical stretching sheet in the presence of thermophoresis and chemical reaction, Boundary Value Prob. 2013 1 (2013) 196.
8. M. Mustafa, Cattaneo-Christov heat flux model for rotating flow and heat transfer of upper-convected Maxwell fluid, AIP Adv. 5 (2015) 047109.
9. F. M. Abbasi, S. A. Shehzad, Heat transfer analysis for three-dimensional flow of Maxwell fluid with temperature dependent thermal conductivity: Application of Cattaneo-Christov heat flux model, J. Mol. Liq. 220 (2016) 848-854.
10. K. L. Hsiao, Combined electrical MHD heat transfer thermal extrusion system using Maxwell fluid with radiative and viscous dissipation effects, Appl. Therm. Eng. 112 (2017) 1281-1288.
11. I. Khan, N. A. Shah, L. C. C. Dennis, A scientific report on heat transfer analysis in mixed convection flow of Maxwell fluid over an oscillating vertical plate, Sci. Rep. 77 (2017) 40147.
12. G. K. Ramesh, B. C. Prasannakumara, B. J. Gireesha, S. A. Shehzad, F. M. Abbasi, Three dimensional flow of Maxwell fluid with suspended nanoparticles past a bidirectional porous stretching surface with thermal radiation, Therm. Sci. Eng. Prog. 1 (2017) 6-14.
13. M. Mustafa, T. Hayat, A. Alsaedi, Rotating flow of Maxwell fluid with variable thermal conductivity: an application to non-Fourier heat flux theory, Int. J. Heat & Mass Transf. 106 (2017) 142-148.

14. R. Jusoh, R. Nazar, I. Pop, Flow and heat transfer of magnetohydrodynamic three-dimensional maxwell nanofluid over a permeable stretching/shrinking surface with convective boundary conditions, Int. J. Mech. Sci. 124 (2017) 166-173.
15. M. Mustafa, A. Mushtaq, T. Hayat, A. Alsaedi, Non-aligned MHD stagnation-point flow of upper-convected Maxwell fluid with nonlinear thermal radiation, Neural Comput. Appl. 30 (2018) 1549 –1555.
16. K. Hosseinzadeh, M. Gholinia, B. Jafari, A. Ghanbarpour, H. Olfian, D. D. Ganji, Nonlinear thermal radiation and chemical reaction effects on Maxwell fluid flow with convectively heated plate in a porous medium, Heat Transf.—Asian Res. 48 (2019) 1-16.
17. S. Bilal, K. Ur Rehman, Z. Mustafa, M. Y. Malik, Maxwell nanofluid flow individualities by way of rotating cone, J. Nanofluids 8 (2019) 596-603.
18. A. J. Chamkha, H. S. Takhar, V. M. Soundalgekar, Radiation effects on free convection flow past a semi-infinite vertical plate with mass transfer, Chem. Eng. J. 84 (2001) 335-342.
19. R. Cortell, Similarity solutions for flow and heat transfer of a quiescent fluid over a nonlinearly stretching surface, J. Mater. Process. Technol. 203 (2008) 176-183.
20. K. L. Hsiao, Heat and mass transfer for micropolar flow with radiation effect past a nonlinearly stretching sheet, Heat & Mass Transf. 64 (2010) 413-419.
21. R. Cortell, Heat and fluid flow due to non-linearly stretching surfaces, Appl. Math. Comput. 217 (2011) 7564-7572.
22. K. L. Hsiao, Energy conversion conjugate conduction-convection and radiation over non-linearly extrusion stretching sheet with physical multimedia effects, Energy 59 (2013) 494-502.
23. E. Magyari and A. Pantokratoras, Note on the effect of thermal radiation in the linearized Rosseland approximation on the heat transfer characteristics of various boundary layer flows, Int. Comm. Heat & Mass Transf. 38 (2011) 554-556.
24. A. Pantokratoras, T. Fang, Sakiadis flow with nonlinear Rosseland thermal radiation, Phys. Scr. 87 (2013) 1-5.
25. A. Pantokratoras, T. Fang, Blasius flow with non-linear Rosseland thermal radiation, Meccanica 49 (2014) 1539-1545.

26. D. Pal and P. Saha, Influence of nonlinear thermal radiation and variable viscosity on hydromagnetic heat and mass transfer in a thin liquid film over an unsteady stretching surface, Int. J. Mech. Sci. 119 (2016) 208-216.
27. T. Hayat, M. I. Irfan, M. Waqas, A. Alsaedi, M. Farooq, Numerical simulation for melting heat transfer and radiation effects in stagnation point flow of carbon–water nanofluid, Comp. Meth. Appl. Mech. & Eng. 315 (2018) 1011-1024.
28. F. A. Soomro, R. U. Haq, Q. M. Al-Madallal, Q. Zhang, Heat generation/absorption and nonlinear thermal radiation effect on stagnation point flow of nanofluid along a moving surface, Res. Phys. 8 (2018) 404-414.
29. J. V. R. Reddy, V. Sugunamma, N. Sandeep, Impact of nonlinear radiation on 3D magnetohydrodynamic flow of methanol and kerosene based ferrofluids with temperature dependent viscosity, J. Mol. Liq. 236 (2017) 93–100.
30. M. Mustafa, A. Mushtaq, T. Hayat, A. Alsaedi, Modeling MHD swirling flow due to rough rotating disk with non-linear radiation and chemically reactive solute, Int. J. Num. Meth. Heat & Fluid Flow 28(2018) 2342-2356.
31. M. Mustafa, A. Mushtaq, T. Hayat, A. Alsaedi, Influence of Non-linear Radiation Heat Flux on Rotating Maxwell Fluid over a Deformable Surface: A Numerical Study, Comm. Theo. Phys. 69(2018) 461
32. M. Bilal, M. Sagheer, S. Hussain, Three dimensional MHD upper-convected Maxwell nanofluid flow with nonlinear radiative heat flux, Alexandria Eng. J. 57 (2017) 1917-1925.
33. A. Lopez, G. Ibanez, J. Pantoja, J. Moreira, O. Lastres, Entropy generation analysis of MHD nanofluid flow in a porous vertical microchannel with nonlinear thermal radiation, slip flow and convective-radiative boundary conditions, Int. J. Heat & Mass Transf. 107 (2017) 982-994.
34. M. Mustafa, R. Ahmad, T. Hayat, A. Alsaedi, Rotating flow of viscoelastic fluid with nonlinear thermal radiation: a numerical study, Neural Comput. & Appl. 29 (2018) 493-499.
35. G. Ibáñez, A. López, I. López, J. Pantoja, J. Moreira, O. Lastres, Optimization of MHD nanofluid flow in a vertical microchannel with a porous medium, nonlinear

radiation heat flux, slip flow and convective–radiative boundary conditions, J. Therm. Anal. & Calorim. 135 (2018) 3401-3420.

36. K. B. Lakshmi, K. A. Kumar, J. V. Reddy, V. Sugunamma, Influence of nonlinear radiation and cross diffusion on MHD flow of Casson and Walters-B nanofluids past a variable thickness sheet, J. Nanofluids 8 (2019) 73-83.
37. R. Kumar, R. Kumar, M. Sheikholeslami, A. J. Chamkha, Irreversibility analysis of the three dimensional flow of carbon nanotubes due to nonlinear thermal radiation and quartic chemical reactions, J. Mol. Liq. 274 (2019) 379-392.
38. L.F. Shampine, M.W. Reichelt and J. Kierzenka, Solving boundary value problems for ordinary differential equations in MATLAB with bvp4c; https://www.mathworks.com/help/matlab/ref/bvp4c.html.
39. Solving boundary value problems for ordinary differential equations in MATLAB with bvp4c, Tutorial Notes (2007) 437-438.
40. M. Mustafa, J.A. Khan, T. Hayat, A. Alsaedi, Sakiadis flow of Maxwell fluid considering magnetic field and convective boundary conditions, AIP. Adv. 5 (2015) 027106.
41. R. Cortell, A numerical tackling on Sakiadis flow with thermal radiation, Chin. Phys. Lett. 25 (2008) 1340-1342.
42. S. Rosseland, Astrophysik and atom-theoretische Grundlagen, Springer-Verlag, Berlin, (1931) 41–44.